International Journal of Fracture **109:** 239–261, 2001.

Transient response of a surface crack subjected to dynamic anti-plane concentrated loadings

YI-SHYONG ING[1] and CHIEN-CHING MA[2]
[1]*Department of Aerospace Engineering Tamkang University Tamsui, Taipei, Taiwan 251, R.O. China*
[2]*Department of Mechanical Engineering National Taiwan University Taipei, Taiwan 106, R.O. China*

Received 24 August 1999; accepted in revised form 1 November 2000

Abstract. In this study, the transient response of a surface crack in an elastic solid subjected to dynamic anti-plane concentrated loadings is investigated. The angles of the surface crack and the half-plane are 60° and 90°. In analyzing this problem, an infinite number of diffracted and reflected waves generated by the crack tip and edge boundaries must be taken into account and it will make the analysis extremely difficult. The solutions are determined by superposition of the proposed fundamental solution in the Laplace transform domain and by using the method of image. The fundamental solution to be used is the problem for applying exponentially distributed traction on the crack faces. The exact transient solutions of dynamic stress intensity factor are obtained and expressed in formulations of series form. The solutions are valid for an infinite length of time and have accounted for the contribution of an infinite number of diffracted waves. The explicit value of the dynamic overshot for the perpendicular surface crack is obtained from the analysis. Numerical results are evaluated which indicate that the dynamic stress intensity factors will oscillate near the correspondent static values after the first three or six waves have passed the crack tip.

Key words: Dynamic fracture, dynamic overshot, stress intensity factor, surface crack, transient analysis, wave propagation.

1. Introduction

From the late nineteenth century, the study of stress concentration of an elastic body with cracks, cavities, inclusions, or other types of discontinuities is the major subject of the elastostatics. The question on whether the static stress intensity factors are applicable to dynamic response was not answered before the phenomenon of scattering of elastic waves was recognized in the late 1950s. In general, the dynamic stress intensity factors are much greater than the corresponding static values such that the inertia effects of structures can not be neglected in many dynamic designs, for examples aircraft, vessels, and nuclear plants, etc. Hence the investigation of dynamic fracture problems has become more important and has received much attention by many researchers.

Most of the work for dynamic fracture analysis, however, has been directed towards the solutions of problems without any characteristic length. The complete solutions of this kind of problems can be obtained by integral transform methods in conjunction with direct application of the Wiener-Hopf technique (Noble, 1958) and the Cagniard-de Hoop method (de Hoop, 1958) of Laplace inversion. If the cracked problem has a characteristic length or the loading condition is unsymmetry, then the same procedure using integral transform methods is hard to apply. The problem of an elastic solid containing a semi-infinite crack subjected to a pair of concentrated point loadings on the crack faces has been previously studied by Freund (1974).

He proposed a fundamental solution arising from an edge dislocation climbing along the line ahead of the crack tip with a constant speed to overcome these difficulties of the case with a characteristic length. Basing the procedure on this method, Brock (1982, 1984), Brock et al. (1985), and Ma and Hou (1990, 1991) have analyzed a series of problems of an unbounded medium containing a semi-infinite crack subjected to impact loading. The limitation of above-mentioned problems is that the incident field must be represented as a function of $f(t/x)$, say self-similar. For problems of non-infinite domain or with complicated loading conditions, the solutions can not be obtained by using this method. Exact transient closed form solutions for a stationary semi-infinite crack subjected to a suddenly applied dynamic body force in an unbounded medium have been obtained by Tsai and Ma (1992) for the in-plane case and by Ma and Chen (1993) for the anti-plane case. They determined the solutions by superimposing a fundamental solution in the Laplace transform domain. This is the first time to obtain the solution of a cracked problem subjected to a cylindrical incident field. The advantages of the superposition method in the transform domain were fully indicated in solving these problems. This fundamental solution has also successfully been applied to solve the problem of a half plane containing a semi-infinite inclined crack by Tsai and Ma (1993), but only the first contribution of the incident wave at the crack tip was obtained.

The stress intensities at the edges of a finite crack subjected to time-harmonic, horizontally polarized plane wave have been obtained by Loeber and Sih (1968) and Sih and Loeber (1968, 1969). Thau and Lu (1971), following the work of Kostrov (1964) and Flitman (1963), treated the analogous transient problem of diffraction of an arbitrary plane dilatational wave by a finite crack in an infinite elastic solid. Their results are exact only at the time interval that the dilatational wave has travelled the length of the crack twice. Sih and Embley (1972) have studied the near field solution for the problem of a finite crack under transient in-plane loading. He reduced the mixed boundary value problem to a standard Fredholm integral equation and subsequently inverted the Laplace transform of the stress components by a combination of numerical means and an application of the Cagniard inversion technique. A class of problems involving interaction between a finite crack and other boundaries was considered by Chen (1977, 1978) and Itou (1980, 1981). With the exception of Loeber and Sih (1968) who considered the time-harmonic incident wave, all of the authors mentioned above have simplified their problems by assuming the symmetry distributed loading conditions, and finally used a numerical Laplace inversion technique to obtain the solutions in the physical domain. Because of the mathematical difficulties, the transient close form analytical solution for the problem of a finite crack loaded by an arbitrary located dynamic loading has not been attempted until Ing and Ma (1996, 1997) proposed a useful fundamental solution to overcome this difficulty. Ing and Ma (1996, 1997) used the fundamental solution of a dislocation type to solve the problem of a finite crack subjected to a dynamic anti-plane point loading and a horizontally polarized shear wave.

In this study, the transient response of a surface crack subjected to dynamic anti-plane point loadings is investigated. The inclined angle of the surface crack is chosen to be 600 or 900. In analyzing this problem, the interaction of the crack tip and edge boundaries must be taken into account which makes the analysis extremely difficult. It is impossible to solve this complicated problem by using the standard Wiener-Hopf technique and other approach must be followed. The fundamental solution proposed by Ing and Ma (1996, 1997) is used to solve the problem of multiple diffraction at the crack tip. Furthermore, the reflection generated from the edge boundaries is obtained by using the method of image. Compact and explicit close form solutions are obtained and each term expressed in the solution has its own physical

meaning. Since the stress intensity factor is the key parameter in characterizing dynamic crack growth, we will focus our attention mainly on the determination of the dynamic stress intensity factor.

2. Required fundamental solution

Consider the fundamental problem of an anti-plane deformation for a semi-infinite crack contained in an unbounded medium. The infinite cracked-body is made of an isotropic, homogeneous, and linearly elastic material. The governing equation is represented by the two-dimensional wave equation

$$\frac{\partial^2 w(x, y, t)}{\partial x^2} + \frac{\partial^2 w(x, y, t)}{\partial y^2} - b^2 \frac{\partial^2 w(x, y, t)}{\partial t^2} = 0, \tag{1}$$

where w is the out-of-plane displacement and b is the slowness of the shear wave given by

$$b = \frac{1}{c_s} = \sqrt{\frac{\rho}{\mu}}. \tag{2}$$

Here c_s is the shear wave speed, μ and ρ are the shear modulus and the mass density of the material, respectively. The nonvanishing shear stresses are

$$\tau_{yz} = \mu \frac{\partial w}{\partial y}, \quad \tau_{xz} = \mu \frac{\partial w}{\partial x}. \tag{3}$$

The solution for an exponentially distributed loading applied at the crack faces in the Laplace transform domain will be referred to as the fundamental solution. The problem can be viewed as a half-plane problem with the material occupying the region $y \geq 0$, subjected to the following mixed boundary conditions in the Laplace transform domain

$$\overline{\tau}_{yz}(x, 0, s) = e^{s\eta x} \quad \text{for} \quad -\infty < x < 0, \tag{4}$$

$$\overline{w}(x, 0, s) = 0 \quad \text{for} \quad 0 < x < \infty, \tag{5}$$

where s is the Laplace transform parameter and η is a constant. The overbar symbol is used for denoting the transform on time t. *The one-sided Laplace transform with respect to time and the two-sided Laplace transform with respect to x are defined by*

$$\overline{w}(x, y, s) = \int_0^\infty w(x, y, t) e^{-st} \mathrm{d}t, \tag{6}$$

$$\overline{w}^*(\lambda, y, s) = \int_{-\infty}^\infty \overline{w}(x, y, t) e^{-s\lambda x} \mathrm{d}t. \tag{7}$$

The solution of the proposed fundamental problem can be obtained in the usual way by making use of integral transform methods. Apply a one-sided Laplace transform with respect to t and a two-sided Laplace transform with respect to x on (1). General solution in the transform domain, which are bounded as $y \to +\infty$, can be expressed as

$$\overline{w}^*(\lambda, y, s) = A(s, \lambda) e^{-s\beta(\lambda) y}, \tag{8}$$

where

$$\beta(\lambda) = \sqrt{b+\lambda} \cdot \sqrt{b-\lambda} = \beta_+(\lambda) \cdot \beta_-(\lambda), \tag{9}$$

and A is an unknown function. The branch cuts of $\beta(\lambda)$, *are introduced to ensure* $Re(\beta) \geq 0$ *in the entire cut complex* λ*-plane, where "Re" denotes the real part.*

Application of the Laplace transforms to the boundary conditions (4) and (5) yields

$$\overline{\tau}^*_{yz}(\lambda, 0, s) = \frac{1}{s(\eta-\lambda)}) + \overline{\tau}^*_{yz+}, \quad -\infty < x < \infty \tag{10}$$

$$\overline{w}^*(\lambda, 0, s) = \overline{w}^*_-, \quad -\infty < x < \infty, \tag{11}$$

where $Re(\eta) > Re(\lambda)$ *and* $\overline{\tau}^*_{yz+}$ *is defined to be the twice Laplace transform result of the unknown shear stress* τ_{yz} *on the plane* $y = 0$ *for* $0 < x < \infty$. *Likewise, the function* $\overline{w}^*_-$ *is the transformed result of the unknown displacement* w_- *of the crack face* $y = 0^+$ *in the* z *direction for* $-\infty < x < 0$.

By using the stress-displacement relation in Equation (3) and substituting Equation (8) into the boundary conditions in Equations (10) and (11) along the crack line $y = 0$ *yields*

$$-\mu s\beta(\lambda)\overline{w}^*_- = \frac{1}{s(\eta-\lambda)}) + \overline{\tau}^*_{yz+}. \tag{12}$$

From the general Wiener-Hope technique (Noble, 1958), the splitting can be performed as

$$-\mu s\beta(\lambda)\overline{w}^*_- - \frac{1}{s\beta_+(\eta)(\eta-\lambda)} = \frac{1}{s(\eta-\lambda)}\left[\frac{1}{\beta_+(\lambda)} - \frac{1}{\beta_+(\eta)}\right] + \frac{\overline{\tau}^*_{yz+}}{\beta_+(\lambda)}. \tag{13}$$

The left-hand side of this equation is regular for $\mathrm{Re}(\lambda) < 0$, *while the right-hand side is regular for* $\mathrm{Re}(\lambda) > -b$. *Applying the analytic continuation argument, therefore, each side of Equation (13) represents one and the same entire function, say* $E(\lambda)$. *By Liouville's theorem, the bounded entire function* $E(\lambda)$ *is a constant. The magnitude of the constant can be obtained from order conditions on* $E(\lambda)$ *as* $|\lambda| \to \infty$, *which in turn are obtained from order conditions on the dependent field variables in the vicinity of* $x = 0$. *Furthermore,* $\overline{w}_-$ *is expected to vanish as* $x \to 0^-$ *to ensure continuity of displacement, and* $\overline{\tau}_{xy+}(x, 0, s)$ *is expected to be square root singular as* $x \to 0^+$ *for the stationary crack case. Consequently from the Abel theorem,* $E(\lambda)$ *vanishes completely and then from Equation (13), we find*

$$\overline{w}^*_- = \frac{-1}{\mu s^2\beta_+(\eta)(\eta-\lambda)\beta_-(\lambda)} = A. \tag{14}$$

In view of Equations (3), (8), and (11), inverting the two-sided Laplace transform, we obtain the solutions of stresses and displacement for the fundamental problem in the Laplace transform domain as follows

$$\overline{\tau}_{yz}(x, y, s) = \frac{1}{2\pi i}\int_{\Gamma_\lambda} \frac{(b+\lambda)^{1/2}e^{-s(\beta y-\lambda x)}}{(b+\eta)^{1/2}(\eta-\lambda)}\,\mathrm{d}\lambda, \tag{15}$$

$$\overline{\tau}_{xz}(x, y, s) = \frac{-1}{2\pi i}\int_{\Gamma_\lambda} \frac{\lambda e^{-s(\beta y-\lambda x)}}{(b+\eta)^{1/2}(\eta-\lambda)(b-\lambda)^{1/2}}\,\mathrm{d}\lambda, \tag{16}$$

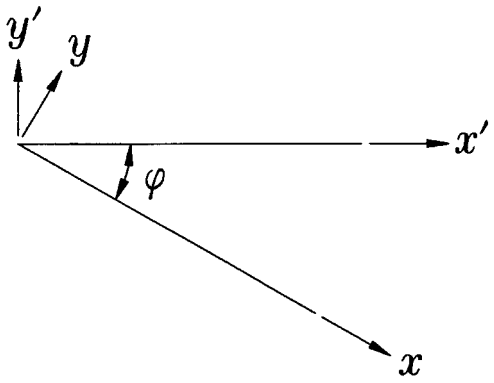

Figure 1. Configuration and coordinate systems of an elastic wedge of apex angle φ.

$$\overline{w}(x, y, s) = \frac{-1}{2\pi i} \int_{\Gamma_\lambda} \frac{e^{-s(\beta y - \lambda x)}}{\mu s (b + \eta)^{1/2} (\eta - \lambda)(b - \lambda)^{1/2}} \, d\lambda, \tag{17}$$

in which Γ_λ is the usual inversion path for the two-sided Laplace transform from $\lambda_1 - i\infty$ to $\lambda_1 + i\infty$, and λ_1 is a real number located in the interval $|\lambda_1| < b$.

The corresponding result of dynamic stress intensity factor in the Laplace transform domain

$$\overline{K}(s) = \lim_{x \to 0} \sqrt{2\pi x} \overline{\tau}_{yz}(x, 0, s) = -\frac{\sqrt{2}}{\sqrt{s}(b + \eta)^{1/2}}. \tag{18}$$

3. Stress transformation relation between two coordinate systems

In order to perform the superposition for the surface crack problem, a transformation relation between different coordinate systems should be established first. The stresses in one coordinate system must be transformed to the other such that it has the same coordinate definition as indicated in the fundamental problem, and then the superposition can be applied directly. Consider an elastic wedge of apex angle φ as shown in Figure 1. Two rectangular coordinate systems (x, y) and (x', y') are established such that the x- and x'-axes lie along the two different straight boundaries of the wedge, respectively. The geometric relations between these two coordinate systems can be written as follows

$$x = x' \cos\varphi - y' \sin\varphi, \tag{19}$$

$$y = x' \sin\varphi + y' \cos\varphi, \tag{20}$$

and the nonvanishing shear stresses of the anti-plane problem can be connected by

$$\overline{\tau}_{x'z'} = \overline{\tau}_{xz} \cos\varphi - \overline{\tau}_{yz} \sin\varphi, \tag{21}$$

$$\overline{\tau}_{y'z'} = -\overline{\tau}_{xz} \sin\varphi + \overline{\tau}_{yz} \cos\varphi. \tag{22}$$

Suppose the shear stress $\overline{\tau}_{yz}$ represented in the Laplace transform for the (x, y) coordinate system has the following form

$$\overline{\tau}_{yz}(x, y, s) = \frac{1}{2\pi i} \int_{\Gamma_\lambda} A(s, \lambda) e^{-s\beta y + s\lambda x} \, d\lambda. \tag{23}$$

The other shear stress $\overline{\tau}_{xz}$ is expressed as

$$\overline{\tau}_{xz}(x, y, s) = \frac{-1}{2\pi i} \int_{\Gamma_\lambda} \frac{\lambda A(s, \lambda)}{\beta(\lambda)} e^{-s\beta y + s\lambda x} \, \mathrm{d}\lambda. \tag{24}$$

By using Equations (19) to (22), the shear stress represented in Equation (23) can be transformed to the (x', y') coordinate system and yields

$$\overline{\tau}_{y'z'}(x', y', s) = \frac{1}{2\pi i} \int_{\Gamma_\lambda} A(s, \lambda) M(\lambda) e^{-sT(\lambda)y' + sN(\lambda)x'} \, \mathrm{d}\lambda. \tag{25}$$

in which

$$M(\lambda) = \cos\varphi + \frac{\lambda}{\beta(\lambda)} \sin\varphi, \tag{26}$$

$$T(\lambda) = \beta(\lambda) \cos\varphi + \lambda \sin\varphi, \tag{27}$$

$$N(\lambda) = -\beta(\lambda) \sin\varphi + \lambda \cos\varphi. \tag{28}$$

From the above three equations, we can find the following relations

$$M \, \mathrm{d}\lambda = \mathrm{d}N, \tag{29}$$

$$T = \sqrt{b^2 - N^2} = \beta(N), \tag{30}$$

$$\lambda = N \cos\varphi \pm \sin\varphi \sqrt{b^2 - N^2}. \tag{31}$$

So Equation (25) becomes

$$\begin{aligned} \overline{\tau}_{y'z'}(x', y', s) \; = \; & \frac{1}{2\pi i} \int_{\Gamma_N} A(s, \lambda(N)) e^{-s\beta(N)|y'| + sNx'} \, \mathrm{d}N \\ & \frac{1}{2\pi i} \int_{\Gamma_\lambda} A(s, \zeta) e^{-s\beta(\lambda)|y'| + s\lambda x'} \, \mathrm{d}\lambda, \end{aligned} \tag{32}$$

where

$$\zeta \; = \; \lambda \cos\varphi \pm \sin\varphi \sqrt{b^2 - \lambda^2}.$$

Similarly, the shear stress in Equation (24) can be transformed to the (x', y') *coordinate system and the final result is given by*

$$\overline{\tau}_{x'z'}(x', y', s) = \frac{-1}{2\pi i} \int_{\Gamma_\lambda} \frac{\lambda A(s, \zeta)}{\beta(\lambda)} e^{-s\beta(\lambda)|y'| + s\lambda x'} \, \mathrm{d}\lambda. \tag{33}$$

To sum up, if the shear stresses in Equations (23) and (24) are transformed to a (x', y') coordinate system which rotates a counterclockwise angle φ, from the original (x, y) coordinate system, then the transformed results are given by Equations (32) and (33).

4. Stress intensity factor of a surface crack with an inclined angle

In this section, a surface crack subjected to a dynamic concentrated loading acting at a finite distance h from the end of the crack is investigated in detail. We will focus our attention on

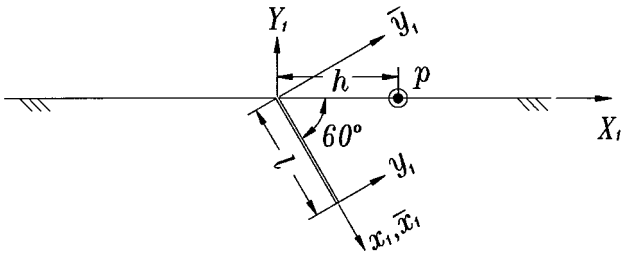

Figure 2. Geometric configuration of a 60° surface crack subjected to a dynamic point loading.

the solution for the dynamic stress intensity factor. Consider an isotropic, homogeneous, and linearly elastic half-plane medium containing a surface crack with finite length l as shown in Figure 2. The angle between the crack tip line and the straight boundary of the half-plane is $\gamma = 60°$. For time $t < 0$, the medium is stress-free and at rest. At time $t = 0$, an anti-plane dynamic concentrated loading of magnitude p acts at $X_1 = h$ on the surface of the half-plane. The time dependence of the loading is represented by the Heaviside step function $\mathrm{H}(t)$. Thus the loading boundary condition can be described as

$$\tau^{i}_{Y_1 Z_1}(X_1, 0, t) = p\delta(X_1 - h)\mathrm{H}(t). \tag{34}$$

This problem involves two characteristic lengths, i.e., l and h, and a direct attempt towards solving this problem by transform methods and Wiener–Hopf techniques is not applicable. Hence the transient elastodynamic problem is solved in this study by superposition of the fundamental solution obtained in Section 2 and by using the method of image. The complete transient solution is composed of an incident field, reflected field, and diffracted field which are denoted by superscripts of i, r, and d, respectively.

Taking the one-sided and two-sided Laplace transforms on Equation (34), the boundary condition becomes

$$\overline{\tau}^{i*}_{Y_1 Z_1}(\lambda, 0, s) = \frac{pe^{-s\lambda h}}{s}. \tag{35}$$

The incident wave of the two-dimensional wave problem must has the form of (similar to Equation (8))

$$\overline{\tau}^{i*}_{Y_1 Z_1}(\lambda, Y_1, s) = B(s, \lambda)e^{s\beta(\lambda)Y_1} \tag{36}$$

which is bounded as $Y_1 \to -\infty$. Substituting Equation (36) into the boundary condition of Equation (35), the unknown function $B(s, \lambda)$ can be obtained and then the incident field is determined. By inverting the two-sided Laplace transform, moreover, the incident field generated by the applying point loading can be expressed in the Laplace transform domain as follows

$$\overline{\tau}^{i}_{Y_1 Z_1}(X_1, Y_1, s) = \frac{1}{2\pi i}\int_{\Gamma_\lambda} pe^{-s\lambda h}e^{s\beta Y_1 + s\lambda X_1}\,\mathrm{d}\lambda, \tag{37}$$

where Γ_λ is the same inversion path as indicated in Equation (15).

In analyzing this complicated problem, it is helpful to observe the phenomenon of wave propagation in a short time period. Figure 3 shows the wave fronts for a short time period after the dynamic point loading is applied. It can be seen in Figure 3 that the first wave arriving at

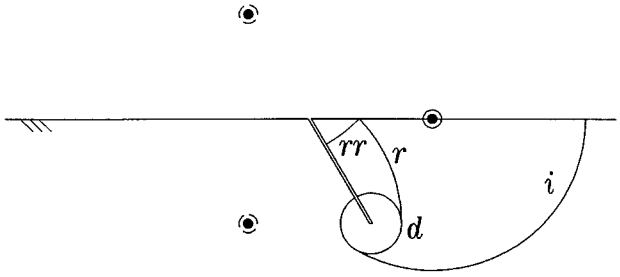

Figure 3. Wave fronts of the incident, reflected, and diffracted waves before *rr* wave arrives at the crack tip.

the crack tip is the incident *i* wave. Furthermore, the second wave reaching the crack tip is the *rr* wave which is induced from the twice reflection of the incident wave between the crack face and the half-plane surface. After a later time, it can be envisaged that only the diffracted *d* (the diffracted wave induced from the incident *i* wave at the crack tip) and *rrd* (the diffracted wave induced from the reflected *rr* wave at the crack tip) waves will be reflected from the traction-free surface of the half-plane and interact with the crack tip. To solve this problem, the diffracted *d* and *rrd* waves should be constructed first. Then the total contribution of the dynamic stress intensity factor which comes from infinite reflections of waves scattered from the crack tip is determined.

Before the *rr* wave arrives the crack tip, the problem is precisely the same as a semi-infinite crack subjected to a dynamic point loading in an infinite medium. Making use of the transformation relation established in the previous section, the incident field represented in Equation (37) can be transformed to (x_1, y_1) coordinate system and the shear stress on the crack face $y_1 = 0$ is given by

$$\overline{\tau}^{i}_{y_1 z_1}(x_1, 0, s) = \frac{1}{2\pi i} \int_{\Gamma_\lambda} p e^{-s\zeta h} e^{s\lambda(x_1 + l)} \, \mathrm{d}\lambda, \tag{38}$$

where

$$\zeta = \lambda \cos\gamma - \beta(\lambda) \sin\gamma.$$

The applied traction on the crack face, in order to eliminate the incident wave as indicated in Equation (38), has the functional form $e^{s\lambda x_1}$. Since the solution for applying traction $e^{s\eta x_1}$ at crack faces has been obtained in Section 2, the reflected and diffracted field can be constructed by superimposing the incident wave traction that is equal and opposite to (38). By combination of Equations (15) and (38), the solution for the diffracted *d* wave can be expressed as follows

$$\overline{\tau}^{d}_{y_1 z_1}(x_1, y_1, s) = \frac{-p}{(2\pi i)^2} \int_{\Gamma_{\eta_1}} \int_{\Gamma_{\eta_2}} G(\eta_1, \eta_2) e^{-s\zeta_1 h + s\eta_1 l - s\beta y_1 + s\eta_2 x_1} \, \mathrm{d}\eta_2 \, \mathrm{d}\eta_1, \tag{39}$$

in which

$$G(\eta_1, \eta_2) = \frac{(b + \eta_2)^{1/2}}{(b + \eta_1)^{1/2}(\eta_1 - \eta_2)},$$

$$\zeta_1 = \eta_1 \cos\gamma - \beta(\eta_1) \sin\gamma.$$

Equation (39) constitutes a double inversion integral where the path Γ_{η_1} *and* Γ_{η_2} *refer to Laplace inversion contours in the* η_1*-plane and the* η_2*-plane, respectively. A detail description*

of the paths of integration and the result of $\tau^{d}_{y_1 z_1}(x_1, y_1, s)$ *can be found in a paper of Ma and Chen (1993, pp. 165–166). The pole contribution* $(\eta_1 = \eta_2)$ *in Equation (39) represents the reflected r wave induced by the traction-free crack faces.*

The corresponding stress intensity factor expressed in the Laplace transform domain is

$$\overline{K}^{d}(s) = \frac{1}{(2\pi i)^2} \int_{\Gamma_\lambda} \frac{\sqrt{2}p}{\sqrt{s}(b+\eta_1)^{1/2}} e^{-s\zeta_1 h + s\eta_1 l}\, \mathrm{d}\eta_1. \tag{40}$$

By using of the Cagniard–de Hoop method of Laplace inversion (cf., Achenbach, 1973, pp. 298–301), the dynamic stress intensity factor at the crack tip induced by the incident wave expressed in time domain can be obtained as follows

$$K^{d}(t) = K^{d,1}(t) = p\sqrt{\frac{2}{\pi r_1}} \sin(\theta_1/2)\mathrm{H}(t - br_1), \tag{41}$$

where

$$r_1 = \left[(h\cos\gamma - l)^2 + h^2 \sin^2\gamma\right]^{1/2}, \qquad \theta_1 = \cos^{-1}\left(\frac{h\cos\gamma - l}{r_1}\right).$$

Expectably, before the arrival of other reflected waves at the crack tip, Equation (41) is the well-known solution for the dynamic stress intensity factor of a semi-infinite crack subjected to a dynamic body force in an unbounded medium.

By application of the method of image (*cf., Achenbach, 1973, pp. 111–113*), it can be seen in Figure 3 that the solution for the *rr* wave is the same as the incident field induced by a point loading applied at $(x_1, y_1) = (-l - h, 0)$. The expression of the shear stress in the Laplace transform domain is given by

$$\overline{\tau}^{rr}_{y_1 z_1}(x_1, 0, s) = \frac{1}{2\pi i} \int_{\Gamma_\lambda} p e^{s\lambda(x_1 + h + l)}\, \mathrm{d}\lambda. \tag{42}$$

When the *rr* wave arrives at the crack tip, the diffracted *rrd* wave will be induced. Using the fundamental solution in Equation (15), the *rrd* wave can be constructed and is given by

$$\overline{\tau}^{rrd}_{y_1 z_1}(x_1, y_1, s) = \frac{p}{(2\pi i)^2} \int_{\Gamma_{\eta_1}} \int_{\Gamma_{\eta_2}} G(\eta_1, \eta_2) e^{s\eta_1(h+l) - s\beta y_1 + s\eta_2 x_1}\, \mathrm{d}\eta_2\, \mathrm{d}\eta_1. \tag{43}$$

Similarly, the corresponding stress intensity factor in the Laplace transform domain can be obtained by combining Equations (18) and (42) and yields

$$\overline{K}^{rrd}(s) = \frac{-1}{2\pi i} \int_{\Gamma_\lambda} \frac{\sqrt{2}p}{\sqrt{s}(b+\lambda)^{1/2}} \mathrm{e}^{s\lambda(h+l)}\, \mathrm{d}\lambda. \tag{44}$$

Applying the inverse Laplace transform to (44), the stress intensity factor in time domain is

$$K^{rrd}(t) = K^{rrd,1}(t) = p\sqrt{\frac{2}{\pi(h+l)}} \mathrm{H}(t - bh - bl). \tag{45}$$

So far we have obtained the first two contributions to the stress intensity factor which are induced by the *d* and *rrd* waves. After a later time, these two waves will be reflected from the traction-free boundary of the half-plane and arrive at the crack tip. Here the effect of the

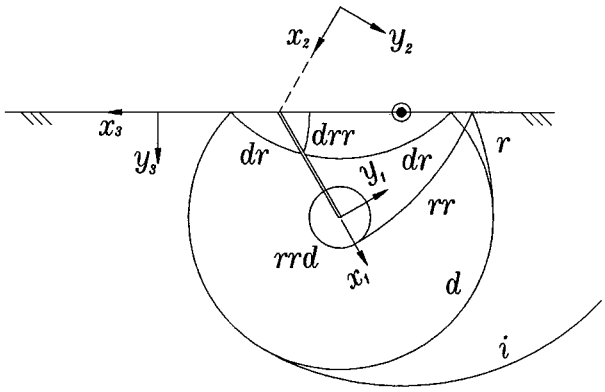

Figure 4. Wave fronts of the incident, reflected, and diffracted fields after the *d* wave has been reflected from the half-plane surface.

d wave is considered first. It can be seen in Figure 4 that the reflected waves of the *d* wave from the comer of the wedge are *dr* and *drr* waves. The *dr* and *drr* waves can be obtained by employing the method of image. *Because the drr wave will not interact with the crack tip, only the dr wave has the contribution of the stress intensity factor at the crack tip.* Using the method of image to Equation (39), the *dr* wave can be obtained as follows

$$\overline{\tau}^{dr}_{y_2z_2}(x_2, y_2, s) = \frac{p}{(2\pi i)^2} \int_{\Gamma_{\eta_1}} \int_{\Gamma_{\eta_2}} G(\eta_1, \eta_2)\, \mathrm{e}^{-s\zeta_1 h + s\eta_1 l - s\beta|y_2| - s\eta_2 x_2}\, \mathrm{d}\eta_2\, \mathrm{d}\eta_1. \tag{46}$$

Equation (46) is transformed to the (x_1, y_1) coordinate system and yields

$$\overline{\tau}^{dr}_{y_1z_1}(x_1, y_1, s) = \frac{p}{(2\pi i)^2} \int_{\Gamma_{\eta_1}} \int_{\Gamma_{\eta_2}} G(\eta_1, -\zeta_2)\, \mathrm{e}^{-s\zeta_1 h + s\eta_1 l - s\beta|y_1 - l'| - s\eta_2(x_1 + l'')}\, \mathrm{d}\eta_2\, \mathrm{d}\eta_1, \tag{47}$$

where

$$\zeta_2 = \eta_2 \cos\gamma - \beta(\eta_2) \sin\gamma,$$

$$l' = l \sin\gamma, \qquad l'' = l + l\cos\gamma.$$

By setting $y_1 = 0$ in Equation (47) and superimposing the fundamental solution in Equation (15), the reflected *drd* wave can be obtained as follows

$$\begin{aligned}\overline{\tau}^{drd}_{y_1z_1}(x_1, y_1, s) \;=\; & \frac{-p}{(2\pi i)^3} \int_{\Gamma_{\eta_1}} \int_{\Gamma_{\eta_2}} \int_{\Gamma_{\eta_3}} G(\eta_1, -\zeta_2) G(\eta_2, \eta_3) \\ & \mathrm{e}^{-s(\zeta_1 h - \eta_1 l) - s(\beta_1 l' - \eta_2 l'') - s\beta|y_1| + s\eta_3 x_1}\, \mathrm{d}\eta_3\, \mathrm{d}\eta_2\, \mathrm{d}\eta_1. \end{aligned} \tag{48}$$

The corresponding stress intensity factor induced by the *drd* wave is

$$\overline{K}^{drd}(s) = \frac{\sqrt{2}p}{(2\pi i)^2} \int_{\Gamma_{\eta_1}} \int_{\Gamma_{\eta_2}} \frac{G(\eta_1, -\zeta_2)}{\sqrt{s}(b + \eta_2)^{1/2}} \mathrm{e}^{-s(\zeta_1 h - \eta_1 l) - s(\beta_1 l' - \eta_2 l'')}\, \mathrm{d}\eta_2\, \mathrm{d}\eta_1. \tag{49}$$

In order to carry out the Laplace inversion of the double integral in Equation (49), the Cagniard contours in both η_1- and η_2-planes are introduced by setting

$$\zeta_1 h - \eta_1 l = t_1, \tag{50}$$

$$\beta(\eta_2)l' - \eta_2 l'' = t_2. \tag{51}$$

Equations (50) and (51) can be solved for η_1 and η_2 to yield

$$\eta_1^{\pm} = \frac{t_1 \cos\theta_1}{r_1} \pm i\frac{\sin\theta_1}{r_1}(t_1^2 - b^2 r_1^2)^{1/2},$$

$$\eta_2^{\pm} = \frac{-t_2 \cos\theta_2}{r_2} \pm i\frac{\sin\theta_2}{r_2}(t_2^2 - b^2 r_2^2)^{1/2},$$

where

$$r_2 = (l' + l'')^{1/2}, \qquad \theta_2 = \cos^{-1}(l''/r_2).$$

In the η_1-plane (or η_2-plane), Equation (50) (or (51)) describes a hyperbola which is denoted as the Cagniard contour. Shifting the η_1 and η_2-integrations onto Cagniard contours along which t_1 and t_2 are both real and positive, the integral variables (η_1 and η_2) in Equation (49) can be changed to t_1 and t_2, respectively, and yield

$$\overline{K}^{drd}(s) = \frac{\sqrt{2}p}{2\pi^2\sqrt{s}} \int_{br_1}^{\infty}\int_{br_2}^{\infty} \mathrm{Re}\left[\frac{G(\eta_1^+, -\zeta_2^+)}{(b+\eta_2^+)^{1/2}}\frac{\partial\eta_1^+}{\partial t_1}\frac{\partial\eta_2^+}{\partial t_2} - \frac{G(\eta_1^-, -\zeta_2^+)}{(b+\eta_2^+)^{1/2}}\frac{\partial\eta_1^-}{\partial t_1}\frac{\partial\eta_2^+}{\partial t_2}\right] \mathrm{e}^{-s(t_1+t_2)}\,\mathrm{d}t_2\,\mathrm{d}t_1. \tag{52}$$

By letting $t_2 = t - t_1$, Equation (52) will become

$$\overline{K}^{drd}(s) = \frac{1}{\sqrt{s}}\int_0^{\infty}\int_{br_1}^{t-br_1} \frac{\sqrt{2}p}{2\pi^2}\mathrm{Re}\left[\frac{G(\eta_1^+, -\zeta_2^+)}{(b+\eta_2^+)^{1/2}}\frac{\partial\eta_1^+}{\partial t_1}\frac{\partial\eta_2^+}{\partial t_2} - \frac{G(\eta_1^-, -\zeta_2^+)}{(b+\eta_2^+)^{1/2}}\frac{\partial\eta_1^-}{\partial t_1}\frac{\partial\eta_2^-}{\partial t_2}\right] \mathrm{H}(t - t_1 - br_2)\,\mathrm{d}t_1 \mathrm{e}^{-st}\,\mathrm{d}t. \tag{53}$$

It is clearly to see that the integral $\int_0^{\infty}[\cdots]\mathrm{e}^{-st}\,\mathrm{d}t$ in the above equation is just equal to the definition of the Laplace transform on t. So the integrand is exactly represented the inverse result of the integral. Furthermore, by using the convolution theorem, the inversion of Equation (53) can be completed and the stress intensity factor in time domain is obtained as follows

$$K^{drd}(t) = K^{d,2}(t) = \frac{-\sqrt{2}p}{2\pi^{5/2}}\int_{b(r_1+r_2)}^{t}\int_{br_1}^{\tau-br_2}\frac{1}{\sqrt{t-\tau}}\mathrm{Re}\left[\frac{G(\eta_1^+, -\zeta_2^+)}{(b+\eta_2^+)^{1/2}}\frac{\partial\eta_1^+}{\partial t_1}\frac{\partial\eta_2^+}{\partial t_2} - \frac{G(\eta_1^-, -\zeta_2^+)}{(b+\eta_2^+)^{1/2}}\frac{\partial\eta_1^-}{\partial t_1}\frac{\partial\eta_2^+}{\partial t_2}\right]_{t=\tau} \mathrm{d}t_1\,\mathrm{d}\tau, \tag{54}$$

where

$$\zeta_2^{\pm} = \eta_2^{\pm}\cos\gamma - \beta(\eta_2^{\pm})\sin\gamma.$$

Similarly, the *drd* wave will be reflected by the traction-free boundary again and reflected *drdr* wave will be generated. The stress intensity factor induced by this reflected wave can be constructed by the same procedure as indicated previously and the result is given as follows

$$K^{drdrd}(t) = K^{d,3}(t) = \frac{-\sqrt{2}p}{4\pi^{7/2}}\int_{b(r_1+2r_2)}^{t}\int_{br_1}^{\tau-2br_2}\int_{br_2}^{\tau-t_1-br_2}\frac{1}{\sqrt{t-\tau}}\mathrm{Im}\,(A_{11} - A_{12} + A_{13} - A_{14})_{t=\tau}\,\mathrm{d}t_2\,\mathrm{d}t_1\,\mathrm{d}\tau, \tag{55}$$

where

$$A_{11} = \frac{1}{(b+\eta_3^+)^{1/2}} G(\eta_1^+, -\zeta_2^+) G(\eta_2^+, -\zeta_3^+) \frac{\partial \eta_1^+}{\partial t_1} \frac{\partial \eta_2^+}{\partial t_2} \frac{\partial \eta_3^+}{\partial t_3},$$

$$A_{12} = \frac{1}{(b+\eta_3^+)^{1/2}} G(\eta_1^+, -\zeta_2^-) G(\eta_2^-, -\zeta_3^+) \frac{\partial \eta_1^+}{\partial t_1} \frac{\partial \eta_2^-}{\partial t_2} \frac{\partial \eta_3^+}{\partial t_3},$$

$$A_{13} = \frac{1}{(b+\eta_3^+)^{1/2}} G(\eta_1^-, -\zeta_2^+) G(\eta_2^+, -\zeta_3^+) \frac{\partial \eta_1^-}{\partial t_1} \frac{\partial \eta_2^+}{\partial t_2} \frac{\partial \eta_3^+}{\partial t_3},$$

$$A_{14} = \frac{1}{(b+\eta_3^+)^{1/2}} G(\eta_1^-, -\zeta_2^-) G(\eta_2^-, -\zeta_3^+) \frac{\partial \eta_1^-}{\partial t_1} \frac{\partial \eta_2^-}{\partial t_2} \frac{\partial \eta_3^+}{\partial t_3},$$

$$\eta_3^{\pm} = \frac{-t_3 \cos\theta_2}{r_2} \pm i \frac{\sin\theta_2}{r_2} (t_3^2 - b^2 r_2^2)^{1/2},$$

$$\zeta_3^{\pm} = \eta_3^{\pm} \cos\gamma - \beta(\eta_3^{\pm}) \sin\gamma.$$

Following the similar procedure, the complete solution for the dynamic stress intensity factor that accounts for the contribution of all the reflected waves originated from the d wave can be obtained. Moreover the contribution of all the reflected waves originated from the rrd wave can be derived in the same way. Finally, the complete solution for the dynamic stress intensity factor of the surface crack can be simplified into a very compact formulation as follows

$$K(t) = \sum_{n=1}^{\infty} K^{d,n}(t) + \sum_{n=1}^{\infty} K^{rrd,n}(t), \tag{56}$$

where

$$K^{d,1}(t) = p\sqrt{\frac{2}{\pi r_1}} \sin(\theta_1/2) \mathrm{H}(t - br_1), \tag{57}$$

$$K^{rrd,1}(t) = p\sqrt{\frac{2}{\pi(h+l)}} \mathrm{H}(t - bh - bl), \tag{58}$$

$$K^{d,n}(t) = \frac{-\sqrt{2}p}{2^{n-1}\sqrt{\pi}\pi^n} \int_{b[r_1+(n-1)r_2]}^{t} \int_{br_1}^{a_1} \int_{br_2}^{a_2} \cdots \int_{br_2}^{a_{n-1}} \frac{SIF_{d,n}}{\sqrt{t-\tau}} \, \mathrm{d}t_n \, \mathrm{d}t_{n-1} \cdots \mathrm{d}t_1 \, \mathrm{d}\tau,$$
$$\text{for } n = 2, 3, 4, \ldots,$$

$$K^{rrd,n}(t) = \frac{-\sqrt{2}p}{\sqrt{\pi}\pi^n} \int_{b[h+l+(n-1)r_2]}^{t} \int_{b(h+l)}^{a_1} \int_{br_2}^{a_2} \cdots \int_{br_2}^{a_{n-1}} \frac{SIF_{rrd,n}}{\sqrt{t-\tau}} \, \mathrm{d}t_n \, \mathrm{d}t_{n-1} \cdots \mathrm{d}t_1 \, \mathrm{d}\tau,$$
$$\text{for } n = 2, 3, 4, \ldots,$$

and

$$a_1 = \tau - (n-1)br_2,$$

$$a_j = \tau - t_1 - t_2 - \cdots - t_{j-1} - (n-j)br_2, \qquad j = 2, 3, \ldots, n,$$

$$t_1 + t_2 + t_3 + \cdots + t_n = t,$$

$$SIF_{d,n} = Op\left[\frac{1}{(b+\eta_n^+)^{1/2}} G(\eta_1^{\pm}, -\zeta_2^{\pm}) G(\eta_2^{\pm}, -\zeta_3^{\pm}) \cdots G(\eta_{n-2}^{\pm}, -\zeta_{n-1}^{\pm}) \times G(\eta_{n-1}^{\pm}, -\zeta_n^{+}) \frac{\pm\partial\eta_1^{\pm}}{\partial t_1} \frac{\pm\partial\eta_2^{\pm}}{\partial t_2} \cdots \frac{\pm\partial\eta_{n-1}^{\pm}}{\partial t_{n-1}} \frac{\partial\eta_n^{+}}{\partial t_n}\right],$$

$$SIF_{rrd,n} = Op\left[\frac{1}{(b+\eta_n^+)^{1/2}} G(\eta_1^{+}, -\zeta_2^{+}) G(\eta_2^{+}, -\zeta_3^{+}) \cdots G(\eta_{n-2}^{+}, -\zeta_{n-1}^{+}) \times G(\eta_{n-1}^{+}, -\zeta_n^{+}) \frac{\partial\eta_1^{+}}{\partial t_1} \frac{\partial\eta_2^{+}}{\partial t_2} \cdots \frac{\partial\eta_{n-1}^{+}}{\partial t_{n-1}} \frac{\partial\eta_n^{+}}{\partial t_n}\right]_{\eta_1^+ = \lambda_1^+},$$

in which

$$G(\eta_1, \eta_2) = \frac{(b+\eta_2)^{1/2}}{(b+\eta_1)^{1/2}(\eta_1 - \eta_2)},$$

$$Op = \mathrm{Re} \quad \text{when } n = 2, 4, 6, \cdots; \qquad Op = \mathrm{Im} \quad \text{when } n = 3, 5, 7, \cdots,$$

$$\eta_1^{\pm} = \frac{t_1 \cos\theta_1}{r_1} \pm i \frac{\sin\theta_1}{r_1} (t_1^2 - b^2 r_1^2)^{1/2},$$

$$\eta_n^{\pm} = \frac{-t_n \cos\theta_2}{r_2} \pm i \frac{\sin\theta_2}{r_2} (t_n^2 - b^2 r_2^2)^{1/2}, \quad \text{for } n = 2, 3, 4, \cdots,$$

$$\zeta_n^{\pm} = \eta_n^{\pm} \cos\gamma - \beta(\eta_n^{\pm}) \sin\gamma,$$

$$\lambda_1^{+} = \frac{-t_1}{h+l} + i\varepsilon,$$

$$r_1 = \left[(h\cos\gamma - l)^2 + h^2 \sin^2\gamma\right]^{1/2}, \qquad \theta_1 = \cos^{-1}\left(\frac{h\cos\gamma - l}{r_1}\right),$$

$$r_2 = (l' + l'')^{1/2}, \qquad \theta_2 = \cos^{-1}(l''/r_2).$$

The contribution of the transient response for dynamic stress intensity factor which accounts for the multiple wave reflections is expressed in the form of an infinite series as shown in Equation (56). Since the transient solution is exact up to the arrival time of the next wave,

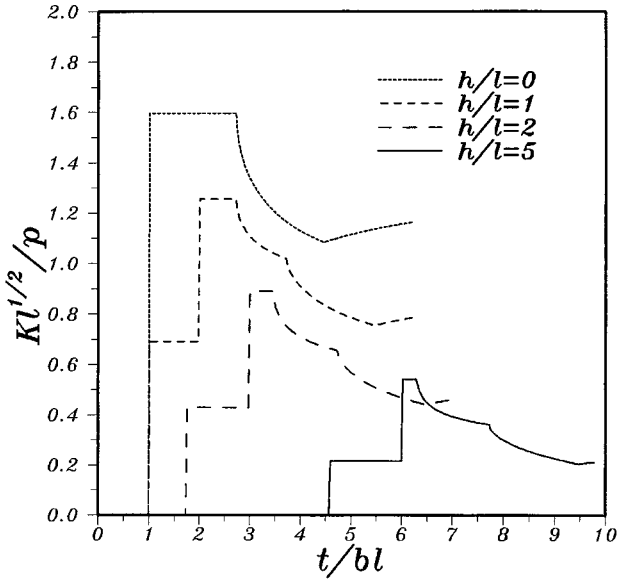

Figure 5. Stress intensity factors of the inclined surface crack for $h/l = 0$, 1, 2, and 5.

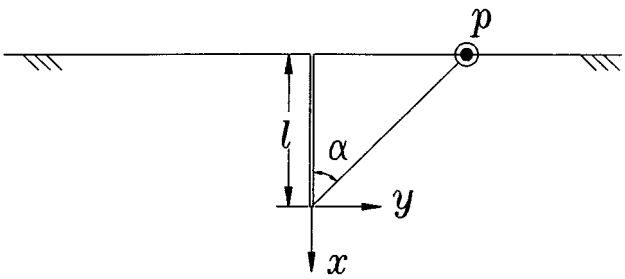

Figure 6. Configuration of a perpendicular surface crack subjected to a dynamic point loading on the half-plane surface.

only a finite number of waves will be involved in the numerical calculation. The numerical calculation includes many high dimensional integrals and it is carried by using the 24-term Gaussian formula. Because the solution for $K^{d,1}(t)$ *(Equation (57)) and* $K^{rrd,1}(t)$ *(Equation (58)) are explicit forms and no integration are involved, the numerical calculation is done only up to three dimensional integral and the corresponding convergence is also checked.* The non-dimensional stress intensity factors $Kl^{1/2}/p$ versus the non-dimensional time t/bl for various values of h/l are shown in Figure 5. It is seen that the dynamic stress intensity factor (except for $h/l = 0$) will reach a peak value when the incident i wave arrives at the crack tip and will raise to another higher peak value when the reflected rr wave arrives at the crack tip, and then decrease to the value near the first peak and finally oscillates near some constant value after the first six waves have passed through the crack tip. Also it is noted that the constant value is higher than the first peak but smaller than the second one. It means that the maximum dynamic overshot always occurs at the instance that the rr wave arrives at the crack tip.

5. A perpendicular surface crack subjected to point loading on half-plane surface

In the previous section, we have derived the analytic solution of the dynamic stress intensity factor of an inclined surface crack subjected to a dynamic concentrated loading on the surface of the half-plane. In the following sections, we will consider the surface-crack problems which contain cracks perpendicular to the boundary. In this section, a perpendicular surface crack subjected to a dynamic point loading on the traction-free boundary of the half-plane as shown in Figure 6 will be discussed. The length of the surface crack is l and the angle of the loading and the negative x-axis is α. Following the similar procedure as indicated in the previous section and using the fundamental solution of dislocation type proposed by Ing and Ma (1996), the stress intensity factor for this perpendicular crack can be constructed. The final solution can be expressed in a compact formulation as follows

$$K(t) = \sum_{n=1}^{\infty} K^{dn}(t), \tag{59}$$

where

$$K^{d1}(t) = p\sqrt{\frac{2\cos\alpha}{\pi l}}\sin\left(\frac{\pi-\alpha}{2}\right)\mathrm{H}(t - bl\sec\alpha), \tag{60}$$

$$K^{dn}(t) = \frac{\sqrt{2}p(i)^q}{2\sqrt{\pi}\pi^n(i)^n}\int_{bR+2(n-1)bl}^{t}\int_{bR}^{a_1}\int_{2bl}^{a_2}\int_{2bl}^{a_3}\cdots \int_{2bl}^{a_{n-1}}\frac{Op\,[SSIF]_{t=\tau}}{\sqrt{t-\tau}}\,\mathrm{d}t_{n-1}\,\mathrm{d}t_{n-2}\cdots\mathrm{d}t_1\,\mathrm{d}\tau, \quad \text{for } n = 2, 3, 4, \cdots,$$

$$a_1 = \tau - 2(n-1)bl,$$

$$a_\nu = \tau - t_1 - t_2 - \cdots - t_{\nu-1} - 2(n-\nu)bl, \qquad \nu = 2, 3, 4, \cdots, n-1,$$

$$t_1 + t_2 + t_3 + \cdots + t_n = t.$$

$$Op = \mathrm{Re}, \quad q = 0, \qquad \text{when } n = 2, 4, 6, \ldots,$$
$$Op = \mathrm{Im}, \quad q = 1, \qquad \text{when } n = 3, 5, 7, \ldots,$$

$$SSIF = \frac{T(\eta_1^+,\eta_2^+)T(\eta_2^+,\eta_3^+)\cdots T(\eta_{n-1}^+,\eta_n^+)}{(b+\eta_1^+)^{1/2}}\frac{\partial\eta_1^+}{\partial t_1}\frac{\partial\eta_2^+}{\partial t_2}\frac{\partial\eta_3^+}{\partial t_3}\cdots\frac{\partial\eta_n^+}{\partial t_n} - \frac{T(\eta_1^-,\eta_2^+)T(\eta_2^+,\eta_3^+)\cdots T(\eta_{n-1}^+,\eta_n^+)}{(b+\eta_1^-)^{1/2}}\frac{\partial\eta_1^-}{\partial t_1}\frac{\partial\eta_2^+}{\partial t_2}\frac{\partial\eta_3^+}{\partial t_3}\cdots\frac{\partial\eta_n^+}{\partial t_n},$$

$$T(\eta_1,\eta_2) = \frac{(b-\eta_2)^{1/2}}{(\eta_1+\eta_2)(b+\eta_2)^{1/2}},$$

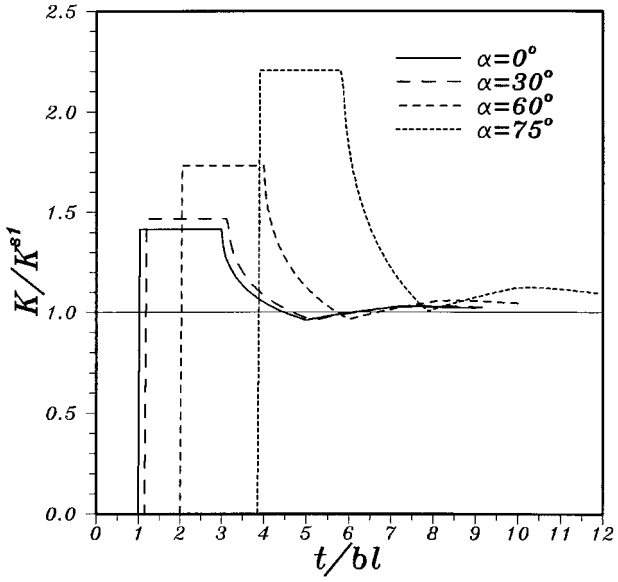

Figure 7. Stress intensity factors for applying dynamic loading on the half-plane surface for $\alpha = 0°$, 30°, 60°, and 75°.

$$\eta_1^{\pm} = \frac{-t_1 \cos\alpha}{R} \pm i \frac{i \sin\alpha}{R}(t_1^2 - b^2 R_2^2)^{1/2},$$

$$\eta_n^{\pm} = \frac{-t_n}{2l} \pm i\varepsilon, \qquad \text{for } n = 2, 3, 4, \ldots,$$

$$R = l \sec\alpha.$$

The corresponding static solution for this case is (Sih, 1965a)

$$K^{s1} = \frac{p \cos\alpha}{\sqrt{\pi l}}. \tag{61}$$

The non-dimensional stress intensity factors K/K^{s1} versus the non-dimensional time t/bl for various values of α are shown in Figure 7. It is indicated in Figure 7 that the dynamic stress intensity factor will reach a peak when the incident wave arrives at the crack tip and then oscillates near the static value after the first three waves have passed through the crack tip. *The dynamic stress intensity factor has only one peak because the r wave reflected by the crack faces will not interact with the crack tip.* Moreover, it can be seen that if the loading is away from the crack tip (i.e., large α), the dynamic overshot will be large. The maximum dynamic overshot always occurs at the time that the incident wave arrives at the crack tip and the ratio of the value for maximum overshot to the static value can be obtained from Equations (60) and (61)

$$\frac{K^{\max}(t)}{K^{s1}} = \sqrt{2 \sec\alpha} \sin\left(\frac{\pi - \alpha}{2}\right). \tag{62}$$

The dynamic overshots for $\alpha = 0°$, 30°, 60° and 75° are $\sqrt{2}$, 1.47, 1.73 and 2.2, respectively.

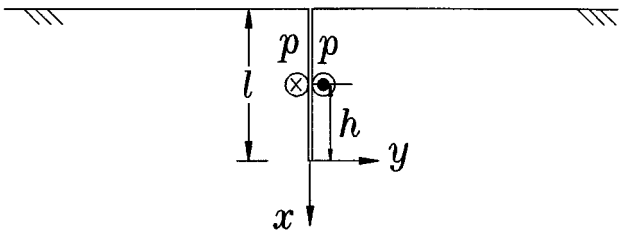

Figure 8. Configuration of a perpendicular surface crack subjected to a pair of dynamic point loadings on crack faces.

6. A perpendicular surface crack subjected to point loadings on crack faces

Consider a perpendicular surface crack with length l which is subjected to a pair of dynamic point loadings on crack faces at a distance h from the crack tip, as shown in Figure 8. By using the similar procedure, the dynamic stress intensity factor of this problem can be obtained as follows

$$K(t) = \sum_{n=1}^{\infty} \sum_{m=0}^{1} K^{m,n}(t), \tag{63}$$

where

$$K^{0,1}(t) = p\sqrt{\frac{2}{\pi h}}\mathrm{H}(t - bh), \tag{64}$$

$$K^{1,1}(t) = p\sqrt{\frac{2}{\pi(2l - h)}}\mathrm{H}(t - 2bl + bh), \tag{65}$$

$$\begin{aligned} K^{0,n}(t) \;=\; & \frac{(-1)^{n-1}\sqrt{2\delta}\,p}{\sqrt{\pi}\pi^n} \int_{b\delta+2(n-1)bl}^{t} \int_{b\delta}^{a_1} \int_{2bl}^{a_2} \cdots \\ & \int_{2bl}^{a_{n-1}} \frac{CSIF0}{\sqrt{t-\tau}}\, \mathrm{d}t_{n-1}\, \mathrm{d}t_{n-2} \cdots \mathrm{d}t_1\, \mathrm{d}\tau, \quad \text{for } n = 2, 3, 4, \cdots, \end{aligned}$$

$$\begin{aligned} K^{1,n}(t) \;=\; & \frac{(-1)^{n-1}\sqrt{2\delta'}\,p}{\sqrt{\pi}\pi^n} \int_{b\delta'+2(n-1)bl}^{t} \int_{b\delta'}^{a_1} \int_{2bl}^{a_2} \cdots \\ & \int_{2bl}^{a_{n-1}} \frac{CSIF1}{\sqrt{t-\tau}}\, \mathrm{d}t_{n-1}\, \mathrm{d}t_{n-2} \cdots \mathrm{d}t_1\, \mathrm{d}\tau, \quad \text{for } n = 2, 3, 4, \cdots, \end{aligned}$$

in which

$$CSIF0 = \left[\frac{\sqrt{t_2 + 2bl} \cdots \sqrt{t_n + 2bl}}{\sqrt{t_1 - b\delta}(2lt_1 + \delta t_2)(t_2 + t_3) \cdots (t_{n-1} + t_n)\sqrt{t_2 - 2bl} \cdots \sqrt{t_n - 2bl}} \right]_{t=\tau},$$

$$CSIF1 = \left[\frac{\sqrt{t_2 + 2bl} \cdots \sqrt{t_n + 2bl}}{\sqrt{t_1 - b\delta'}(2lt_1 + \delta' t_2)(t_2 + t_3) \cdots (t_{n-1} + t_n)\sqrt{t_2 - 2bl} \cdots \sqrt{t_n - 2bl}} \right]_{t=\tau},$$

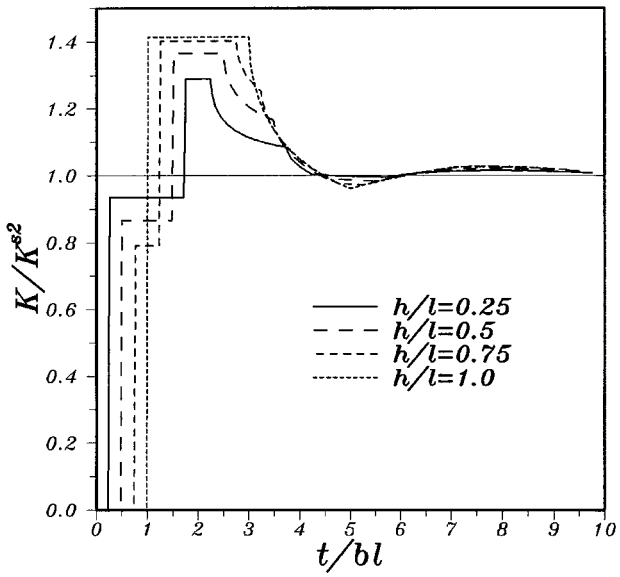

Figure 9. Stress intensity factors for applyitig dynamic loading on the perpendicular surface crack faces for $h/l = 0.25, 0.5, 0.75$, and 1.0.

$$a_1 = \tau - 2(n-1)bl,$$

$$a_\nu = \tau - t_1 - t_2 - \cdots - t_{\nu-1} - 2(n-\nu)bl, \qquad \nu = 2, 3, 4, \ldots n-1,$$

$$\delta = h, \quad \delta' = 2l - h, \qquad \text{when } n = 3, 5, 7, \ldots,$$
$$\delta = 2l - h, \quad \delta' = h, \qquad \text{when } n = 2, 4, 6, \ldots,$$

$$t_1 + t_2 + t_3 + \cdots + t_n = t.$$

The corresponding static solution for this case is (Sih, 1965b)

$$K^{s2} = 2p\sqrt{\frac{l}{\pi h(2l-h)}}. \tag{66}$$

The non-dimensional stress intensity factors K/K^{s2} versus the non-dimensional time t/bl for various values of h/l are shown in Figure 9. It can be seen in Figure 9 that the dynamic stress intensity factor will reach a peak when the incident wave arrives at the crack tip and will raise to another higher peak when the first reflected wave comes to the crack tip, and then oscillates near the static value after the first six waves have passed through the crack tip. It is worthy to note that the first peak is smaller than the corresponding static value while the second one is greater than the static value. Furthermore, it is also indicated that the largest dynamic overshot occurs when $h = l$ and the value of the overshot is $\sqrt{2}$. The maximum dynamic overshots for various values of h/l always occur at the time that the second wave,

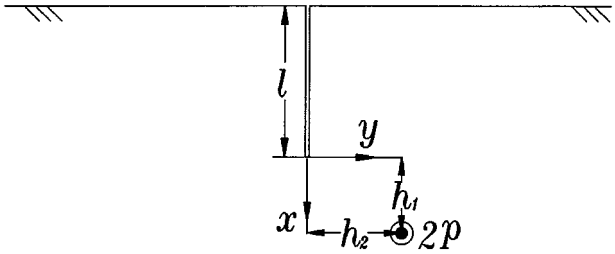

Figure 10. Configuration of a perpendicular surface crack subjected to a dynamic concentrated body force.

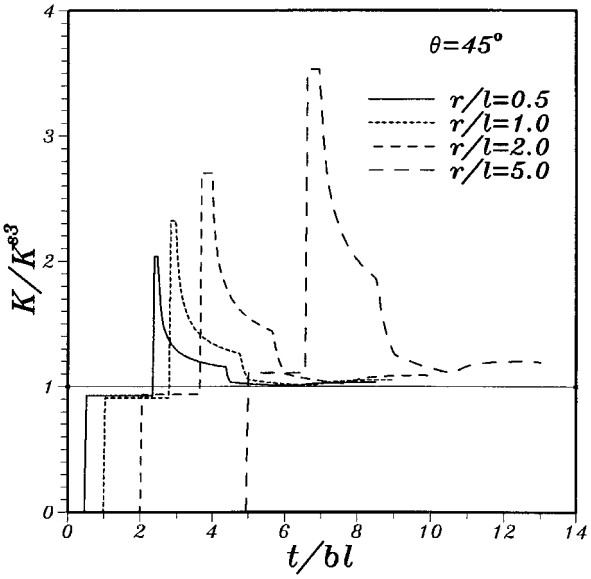

Figure 11. Stress intensity factors of the perpendicular sur face crack subjected to a dynamic body force for $\theta = 45°$ and $r/l = 0.5$, 1.0, 2.0, and 5.0.

i.e., the first reflected wave, arrives at the crack tip and the ratio of the value for maximum overshot to the static value can be obtained from Equations (64) to (66)

$$\frac{K^{\max}(t)}{K^{s2}} = \sqrt{1 - \frac{h}{2l}} + \sqrt{\frac{h}{2l}}. \tag{67}$$

7. A perpendicular surface crack subjected to a dynamic body force

As shown in Figure 10, consider a perpendicular surface crack subjected to a dynamic concentrated anti-plane body force at $x = h_1$, $y = h_2$. The dynamic stress intensity factor can be derived and the result is expressed as follows

$$K(t) = \sum_{n=1}^{\infty} \sum_{m=0}^{1} K^{m,n}(t), \tag{68}$$

where

$$K^{0,1}(t) = p\sqrt{\frac{2}{\pi r}} \sin\left(\frac{\theta}{2}\right) \mathrm{H}(t - br), \tag{69}$$

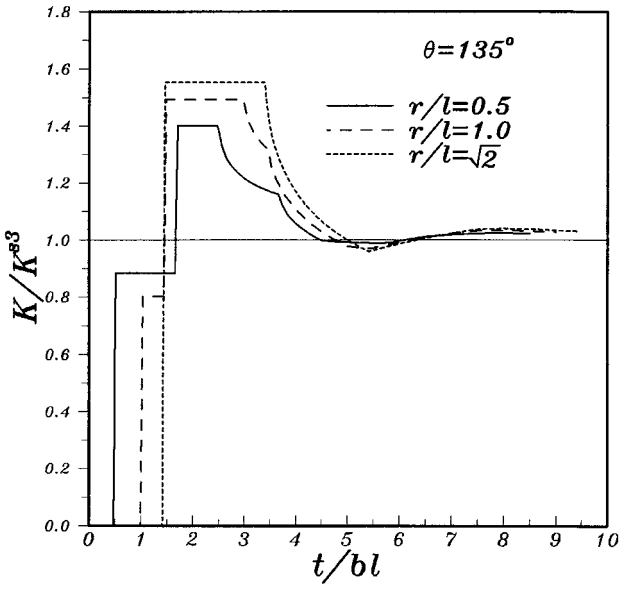

Figure 12. Stress intensity factors of the perpendicular surface crack subjected to a dynamic body force for $\theta = 135°$ and $r/l = 0.5$, 1.0, and $\sqrt{2}$.

$$K^{1,1}(t) = p\sqrt{\frac{2}{\pi r'}}\sin\left(\frac{\pi-\theta'}{2}\right)\mathrm{H}(t-br'), \tag{70}$$

$$K^{0,n}(t) = \frac{\sqrt{2}p(i)^q}{2\sqrt{\pi}\pi^n(i)^n}\int_{br+2(n-1)bl}^{t}\int_{br}^{a_1}\int_{2bl}^{a_2}\int_{2bl}^{a_3}\cdots \int_{2bl}^{a_{n-1}}\frac{Op\,[BSIF]_{t=\tau}}{\sqrt{t-\tau}}\,\mathrm{d}t_{n-1}\,\mathrm{d}t_{n-2}\cdots\mathrm{d}t_1\,\mathrm{d}\tau, \quad \text{for } n=2,3,4,\cdots,$$

$$K^{1,n}(t) = \frac{\sqrt{2}p(i)^q}{2\sqrt{\pi}\pi^n(i)^n}\int_{br'+2(n-1)bl}^{t}\int_{br'}^{a_1}\int_{2bl}^{a_2}\int_{2bl}^{a_3}\cdots \int_{2bl}^{a_{n-1}}\frac{Op\left[BSIF'\right]_{t=\tau}}{\sqrt{t-\tau}}\,\mathrm{d}t_{n-1}\,\mathrm{d}t_{n-2}\cdots\mathrm{d}t_1\,\mathrm{d}\tau, \quad \text{for } n=2,3,4,\cdots,$$

in which

$$a_1 = \tau - 2(n-1)bl,$$

$$a_\nu = \tau - t_1 - t_2 - \cdots - t_{\nu-1} - 2(n-\nu)bl, \qquad \nu = 2,3,4,\cdots,n-1,$$

$$t_1 + t_2 + t_3 + \cdots + t_n = t.$$

$$BSIF = \frac{T(\eta_1^+,\eta_2^+)T(\eta_2^+,\eta_3^+)\cdots T(\eta_{n-1}^+,\eta_n^+)}{(b+\eta_1^+)^{1/2}}\frac{\partial\eta_1^+}{\partial t_1}\frac{\partial\eta_2^+}{\partial t_2}\cdots\frac{\partial\eta_n^+}{\partial t_n} - \frac{T(\eta_1^-,\eta_2^+)T(\eta_2^+,\eta_3^+)\cdots T(\eta_{n-1}^+,\eta_n^+)}{(b+\eta_1^-)^{1/2}}\frac{\partial\eta_1^-}{\partial t_1}\frac{\partial\eta_2^+}{\partial t_2}\cdots\frac{\partial\eta_n^+}{\partial t_n},$$

$$BSIF' = \frac{T(\eta_1'^{+}, \eta_2^{+})T(\eta_2^{+}, \eta_3^{+})\cdots T(\eta_{n-1}^{+}, \eta_n^{+})}{(b+\eta_1'^{+})^{1/2}}\frac{\partial \eta_1'^{+}}{\partial t_1}\frac{\partial \eta_2^{+}}{\partial t_2}\cdots\frac{\partial \eta_n^{+}}{\partial t_n}$$
$$- \frac{T(\eta_1'^{-}, \eta_2^{+})T(\eta_2^{+}, \eta_3^{+})\cdots T(\eta_{n-1}^{+}, \eta_n^{+})}{(b+\eta_1'^{-})^{1/2}}\frac{\partial \eta_1'^{-}}{\partial t_1}\frac{\partial \eta_2^{+}}{\partial t_2}\cdots\frac{\partial \eta_n^{+}}{\partial t_n},$$

$$T(\eta_1, \eta_2) = \frac{(b-\eta_2)^{1/2}}{(\eta_1+\eta_2)(b+\eta_2)^{1/2}},$$

$$\eta_1^{\pm} = \frac{-t_1\cos\theta}{r} \pm i\frac{i\sin\theta}{r}(t_1^2 - b^2r^2)^{1/2},$$

$$\eta_1'^{\pm} = \frac{-t_1\cos(\pi-\theta')}{r'} \pm i\frac{i\sin(\pi-\theta')}{r'}(t_1^2 - b^2r'^2)^{1/2},$$

$$\eta_n^{\pm} = \frac{-t_n}{2l} \pm i\varepsilon, \qquad \text{for } n = 2, 3, 4, \ldots,$$

$$Op = \mathrm{Re}, \quad q = 0, \qquad \text{when } n = 2, 4, 6, \ldots,$$
$$Op = \mathrm{Im}, \quad q = 1, \qquad \text{when } n = 3, 5, 7, \ldots,$$

$$r = \left(h_1^2 + h_2^2\right)^{1/2}, \qquad \theta = \cos^{-1}\left(\frac{h_1}{r}\right),$$

$$r' = \left[(h_1+2l)^2 + h_2^2\right]^{1/2}, \qquad \theta' = \cos^{-1}\left(\frac{h_1+2l}{r'}\right).$$

The corresponding static solution for this case is (Sih, 1965a)

$$K^{s3} = \frac{p(r+r')}{\sqrt{\pi l r r'}}\sin\left(\frac{\theta-\theta'}{2}\right). \tag{71}$$

Figures 11 and 12 show the non-dimensional stress intensity factors K/K^{s3} versus the non-dimensional time t/bl under different values of r/l for $\theta = 45°$ and 135°, respectively. Similarly, it indicates that the dynamic stress intensity factor oscillates near the static value after the first six waves have passed through the crack tip. The maximum dynamic overshot always appears at the time that the second wave (the reflected wave induced from the incident wave by the half-plane surface) arrives at the crack tip. The ratio of the value for maximum overshot to the static value can be obtained from Equations (69) to (71) and is expressed as follows

$$\frac{K^{\max}(t)}{K^{s3}} = \frac{\sqrt{2l}\left(\sqrt{r'}\sin\dfrac{\theta}{2} + \sqrt{r}\sin\dfrac{\pi-\theta'}{2}\right)}{(r+r')\sin\dfrac{\theta-\theta'}{2}}. \tag{72}$$

8. Conclusions

Because of the quick development of the latter-day industries, such as aircraft, ships, nuclear plants, etc., dynamic fracture analyses of structures subjected to impact loading have become more important. Besides, dynamic wave problems play very important roles in the application of earthquake, geology, and nondestructive testing. General theoretical studies all assume that the structure is an infinite medium and the contained crack has a semi-infinite length. The assumption of lacking characteristic length is discrepant to the situation of realistic problems. If there exists some boundaries or the crack has a finite length, the interaction of boundaries and crack will produce infinite reflected and diffracted waves. It will make the analysis extremely difficult and the usual analytic method can not be effectively employed to this kind of problems.

In this study, the transient response of a surface crack with angle 60° and 90° to the half-plane surface is investigated in detail. A fundamental solution is proposed and used to deal with the problem of diffraction at the crack tip. Furthermore, the effect of reflection on the edge boundary is obtained by using the method of image. The dynamic stress intensity factors of the surface crack for different loading locations are obtained and expressed in compact formulations. Each term in the formulations has its own physical meaning. Numerical results for the inclined and perpendicular surface crack are evaluated and discussed in detail. It is indicated that the maximum dynamic overshot always occurs at the instance that the first or second wave arrives at the crack tip. It is also shown that the dynamic stress intensity factor will oscillate near the static value after the first three or six waves have passed through the crack tip. Moreover, the ratio of the value for maximum overshot to the static value is derived for the case of perpendicular crack. The results are very useful for the application of dynamic fracture design.

The theoretical result of transient response for a surface crack is difficult to obtain because of the multiple diffractions due to the finite length of the crack. So far many results for this topic are based on numerical calculations. The fundamental solution and superposition method proposed in this study are successfully used for solving the surface crack problem by analytic investigation. Although only the results for the surface crack with angle 60° or 90° are obtained in this study, the solutions for other cases of special angles ($\gamma = 360°/n$, n is a positive integer) can be constructed by a similar method. Furthermore, the proposed method can be extended to solve more complicated problems which involve interaction of a surface crack with other boundaries.

References

Achenbach, J.D. (1973). *Wave Propagation in Elastic Solids.* North-Holland Publishing Company, New York.

Broek, L.M. (1982). Shear and normal impact loading on one face of a narrow slit. *International Journal of Solids and Structures* **18**, 467–477.

Brock, L.M. (1984). Stresses in a surface obstacle undercut due to rapid indentation. *Journal of Elasticity* **14**, 415–424

Brock, L.M., Jolles, M. and Schroedl, M. (1985). Dynamic impact over a subsurface crack applications to the dynamic tear test. *Journal of Applied Mechanic* **52**, 287–290.

Chen, E.P. (1977). Impact response of a finite crack in a finite strip under anti-plane shear. *Engineering Fracture Mechanic* **9**, 719–724.

Chen, E.P. (1978). Sudden appearance of a crack in a stretched finite strip. *Journal of Applied Mechanics* **45**, 277–280.

de Hoop, A.T. (1958). Representation theorems for the displacement in an elastic solid and their application to elastodynamic diffraction theory. Doctoral dissertation, Technische hogeschool, Delft.

Flitman, L.M. (1963). Waves generated by sudden crack in a continuous elastic medium. *Applied Mathematics and Mechanics (PMM)* **27**, 938–953.

Freund, L.B. (1974). The stress intensity factor due to normal impact loading of the faces of a crack. *International Journal of Engineering Science* **12**, 179–189.

Ing, Y.S. and Ma, C.C. (1996). Transient response of a finite crack subjected to dynamic anti-plane loading. *International Journal of Fracture* **82**, 345–362.

Ing, Y.S. and Ma, C.C. (1997). Dynamic fracture analysis of a finite crack subjected to an incident horizontally polarized shear wave. *International Journal of Solids and Structures* **34**, 895–910.

Itou, S. (1980). Transient response of a finite crack in a strip with stress-free edges. *Journal of Applied Mechanics* **47**, 801–805.

Itou, S. (1981). Transient response of a finite crack in a half plane under impact bad. *Journal of Applied Mechanics* **48**, 534–538.

Kostrov, B.V. (1964). Self-similar problems of propagation of shear cracks. *Applied Mathematics and Mechanics (PMM)* **28**, 1077–1087.

Loeber, J.F. and Sih, G.C. (1968). Diffraction of antiplane shear waves by a finite crack. *Journal of the Acoustical Society of America* **44**, 90–98.

Ma, C.C. and Chen, S.K. (1993). Exact transient analysis of an anti-plane semi-infinite crack subjected to dynamic body forces. *Wave Motion* **17**, 161–171.

Ma, C.C. and Hou, Y.C. (1990). Theoretical analysis of the transient response for a stationary inplane crack subjected to dynamic impact loading. *International Journal of Engineering Science* **28**, 1321–1329.

Ma, C.C. and Hou, Y.C. (1991). Transient analysis for antiplane crack subjected to dynamic loadings. *Journal of Applied Mechanics* **58**, 703–709.

Noble, B. (1958). *The Wiener-Hopf Technique*, Pergamon Press, London.

Sih, G.C. (1965a). Stress distribution near internal crack tips for longitudinal shear problems. *Journal of Applied Mechanics* **32**, 51–61.

Sih, G.C. (1965b). External cracks under longitudinal shear. *Journal of Franklin Institute* **280**, 139–149.

Sih, G.C. and Embley, G.T. (1972). Impact response of a finite crack in plane extension. *International Journal of Solids and Structures* **8**, 977–993.

Sih, G.C. and Loeber, J.F. (1968). Torsional vibration of an elastic solid containing a penny-shaped crack. *The Journal of the Acoustical Society of America* **44**, 1237–1245.

Sih, G.C. and Loeber, J.F. (1969). Wave propagation in an elastic solid with a line of discontinuity or finite crack. *Quarterly of Applied Mathematics* **27**, 193–213.

Thau, S.A. and Lu, T.H. (1971). Transient stress intensity factor for a finite crack in an elastic solid caused by a dilatational wave. *International Journal of Solids and Structures* **7**, 731–750.

Tsai, C.H. and Ma, C.C. (1992). Transient analysis of a semi-infinite crack subjected to a dynamic concentrated forces. *Journal of Applied Mechanic* **59**, 804–811.

Tsai, C.H. and Ma, C.C. (1993). The stress intensity factor of a subsurface inclined crack subjected to dynamic impact loading. *Int. J. Solids Struct.* **30**, 2163–2175.